SSRG International Journal of Electrical and Electronics Engineering
ISSN: 2348-8379/ https://doi.org/10.14445/23488379/IJEEE-V12I1P111

Volume 12 Issue 1, 114-128, January 2025

Original Article

Open-Source SCADA System Implementation for Hybrid Microgrid Management with Renewable Energy Sources

David Juan Cerezo Quina[1], Tadeu Felix Santos[2], Juan Antonio Butron Llamoca[1], German Alberto Echaiz Espinoza[1]*, Andrés Ortiz Salazar[2], Elmer Rolando Llanos Villarreal[3]

[1]*Universidad Nacional de San Agustin de Arequipa, Arequipa, Peru.*
[2]*Federal University of Rio Grande do Norte (DCA-UFRN), Natal 59072-970, RN, Brazil.*
[3]*Federal Rural University of Semi-Arid (DCME-UFERSA), Mossoró 59625-900, RN, Brazil.*

*Corresponding Author : gechaiz@unsa.edu.pe

Received: 08 November 2024 Revised: 10 December 2024 Accepted: 11 January 2025 Published: 25 January 2025

Abstract *- Microgrids are compact energy systems that integrate renewable sources, such as photovoltaic and wind power, to provide sustainable energy solutions. Microgrids require Supervisory Control and Data Acquisition (SCADA) systems to maintain reliable and efficient operation. This paper introduces a novel, cost-effective, open-source SCADA system tailored for microgrid applications. Implemented on a simulated microgrid with renewable energy inputs, the system leverages a Phase-Locked Loop (PLL) synchronization mechanism for seamless grid integration. The system achieves robust data interfacing, real-time monitoring, and historical data archiving using Matlab-Simulink with an OPC Server and SQL database. Comparative analyses with existing SCADA systems demonstrate its superior cost-effectiveness and adaptability, contributing to sustainable energy accessibility in developing regions like Peru.*

Keywords *- Energy management, Microgrid, Open-source software, Renewable energy, SCADA.*

1. Introduction

Microgrids play a pivotal role in the global transition toward sustainable energy. Yet, their adoption in regions like Peru faces several challenges, including high costs, lack of skilled personnel, and insufficient regulatory support. Existing SCADA systems often lack affordability and adaptability, making them inaccessible to communities in developing regions. This research addresses these gaps by proposing an open-source SCADA system designed to reduce implementation costs while maintaining robust functionality. Our system's modular design and adaptability distinguish it from conventional proprietary solutions, enabling broader adoption and fostering energy independence [1].

In response to these pressing issues, this research proposes developing and implementing a cost-effective, free, open-source Supervisory Control and Data Acquisition (SCADA) system specifically tailored for microgrids. The proposed system addresses the economic, technical, and financial barriers that currently impede the widespread adoption of microgrids by providing an accessible solution for their monitoring and control. Additionally, this research will formulate evidence-based strategies to address socio-cultural and awareness-related challenges, thereby fostering public acceptance and facilitating the shift away from fossil fuels. Through this initiative, the research aspires to contribute to the diversification of Peru's energy matrix by promoting the adoption of sustainable energy sources.

The primary objective of this study is to design, develop, and implement a low-cost, open-source SCADA system for microgrid control and monitoring, with the ultimate goal of enhancing microgrid adoption in Peru. The research will focus on simulating some microgrid configurations using the Matlab-Simulink platform to achieve this objective. This will include modeling a microgrid for a residential community and incorporating renewable energy sources, such as solar panels, to assess feasibility and performance. Additionally, a stand-alone microgrid configuration will be simulated, integrating components such as solar panels, a Maximum Power Point Tracking (MPPT) controller, a battery management system, and an inverter to optimize energy management. The study will also simulate the operation of a grid-connected microgrid, focusing on seamless load transfer and synchronization with the main electrical grid.

Following the simulation phase, the development of the SCADA system will proceed. This will involve designing an intuitive user interface for real-time visualization of key microgrid parameters, including power generation, consumption, and storage. Automated control algorithms will be developed to optimize the energy flow within the microgrid and manage its interaction with the grid. The system will also incorporate a secure data logging and reporting mechanism to monitor microgrid performance and support ongoing maintenance.

Once developed, the SCADA system will be validated through a case study in a microgrid environment with a residential setting. Comprehensive user manuals and training materials will be created to facilitate local communities and technical staff's adoption of the system. Finally, the research findings will be disseminated through publications and presentations, contributing to advancing microgrid technology and promoting greater access to sustainable energy solutions in Peru. In addition to this introductory section, this article is divided into 11 sections. Section 1 presents the state of the art of this article. Section 2 presents the related works. Section 3 details the preliminaries. Section 4 describes development and implementation.

Section 5 details microgrid system implementation. Section 6 details a single-phase inverter design with PLL anchoring to the external grid. Section 7 presents the Electrical Network. Section 8 presents OPC communication. Section 9 presents the RapidSCADA Server. Section 10 presents SQL Server and Reporting Services. Section 11 presents the results and discussion. Section 12 concludes and summarizes the achievement of the objectives of the article.

2. Related Works

In section 2, we review several key studies examined during the research related to the development and implementation of SCADA systems for microgrids. Previous studies have explored low-cost SCADA solutions and their applications in microgrids. For example, Vargas-Salgado (2019) implemented a web-based SCADA system for a hybrid renewable energy lab. Ersoy (2023) focused on photovoltaic monitoring in green buildings, while Li (2017) discussed integrating SCADA systems for intelligent microgrid management. Despite their contributions, these systems often lack the scalability and cost-efficiency necessary for broad implementation in developing regions. Our work bridges these gaps, offering an accessible, open-source alternative [2, 3, 5]. A comprehensive literature review on photovoltaic systems' electrical, thermal, and optical modeling has also been conducted. This review examines the key models proposed in the literature for predicting the behavior of photovoltaic systems, emphasizing the importance of accurate modeling for optimizing system performance [4].

3. Preliminaries

3.1. Microgrid Simulation

The system was modeled using Matlab-Simulink to simulate residential microgrid configurations. Parameters, such as solar irradiance (1000 W/m²) and battery capacity (50Ah), were chosen based on real-world data from Peru's energy profiles. The model includes components like photovoltaic panels, MPPT controllers, inverters, and an external grid connection.

3.2. SCADA Architecture

The SCADA system integrates RapidSCADA for data acquisition, visualization, and reporting. An OPC server facilitates communication between Simulink and the SCADA interface. Data is stored in an SQL database, ensuring secure, accessible historical records.

3.3. Sensitivity Analysis

Sensitivity analyses were conducted to assess system robustness under varying solar irradiance and load conditions. Results demonstrate consistent performance, validating the system's adaptability.

3.4. Simulink in MATLAB

Simulink, a simulation and design tool developed by MathWorks, is extensively utilized in engineering for the modeling, simulation, and analysis of dynamic systems. Integrated with MATLAB, Simulink provides an interactive environment that facilitates the design and simulation of complex and multidisciplinary systems. The core premise behind Simulink's popularity in engineering is its ability to represent systems using a block diagram approach, allowing for model-based design of multidomain systems without the necessity of manual coding [7].

This software simplifies the development of complex systems through a model-based design methodology. This approach enables frequent virtual simulations and design validation, essential for ensuring system designs' accuracy and reliability before physical implementation. Additionally, Simulink supports automatic code generation for production in various programming languages, including C, C++, and VHDL, reflecting the premise that automating the transition from model to code can significantly streamline the development process and reduce the potential for human error [7]. Simulink also enables users to explore different design concepts within a multidomain simulation environment. This capability allows for large-scale system simulations using reusable components and libraries, facilitating iterative design and optimization. Furthermore, Simulink supports deploying simulation models across various testing environments, including desktop simulations, real-time testing, and Hardware-in-the-Loop (HIL) scenarios. The underlying assumption here is that comprehensive simulation capabilities are crucial for evaluating and refining system designs under diverse conditions, thereby enhancing the robustness and reliability of the final product [7].

Moreover, Simulink supports Model-Based Systems Engineering (MBSE), which encompasses the entire lifecycle of system development, from requirements capture and system analysis to detailed design, implementation, and testing, all within a systematic and integrated framework. The premise driving this approach is that MBSE, by providing a cohesive and structured process, enhances the efficiency and effectiveness of system development, ensuring that all aspects of the system are considered and optimized throughout the development lifecycle [7].

3.5. Characterization of Electrical Consumption and Calculation of a Photovoltaic Solar Generation System

The characterization process is based on Case 1, as outlined in the document titled "Guide to the Orientation of the Efficient Use of Energy and Energy Diagnosis" produced by the General Energy Efficiency Management [8]. This case study examines a single-family home within the class B economic sector, representing an independent residential unit. The selection of this specific case reflects the premise that homes in this economic category present unique challenges and opportunities for energy efficiency improvements. By focusing on a typical class B home, the study aims to provide insights into the energy consumption patterns and potential efficiency measures applicable to similar households. The key characteristics of this home are detailed in Table 1.

Table 1. Housing characterization

Ambient	Quantity
Bedrooms	2
Bathrooms	2
Courtyards	1
Garage	1
Study room	1
Laundry	1
Living Room, Dining Room	1

Next, we will assess the power requirements needed to meet the daily electrical demand for the most frequently used appliances. This analysis is based on the premise that understanding the power consumption of these commonly utilized devices is essential for accurately estimating the overall energy needs of a household. The relevant power consumption data is summarized in Table 2.

Table 2. Most frequently used artifacts

Type	Description
Refrigerator	350 W
Electric Cooker	7000W
Rice Cooker	1000W
Microwave Kiln	1100W
29" TV	175W
Computer	600W

The reference power will be established by calculating the average of the two highest power demands associated with the electric stove and the microwave oven. This calculation yields a reference power value of 4050W. The underlying assumption is that these two appliances represent the most significant contributors to the household's peak power demand, making their average a reliable indicator for further analysis.

4. Development and Implementation

4.1. Proposed Research Architecture and System Components

The architecture of the proposed research work is detailed below.

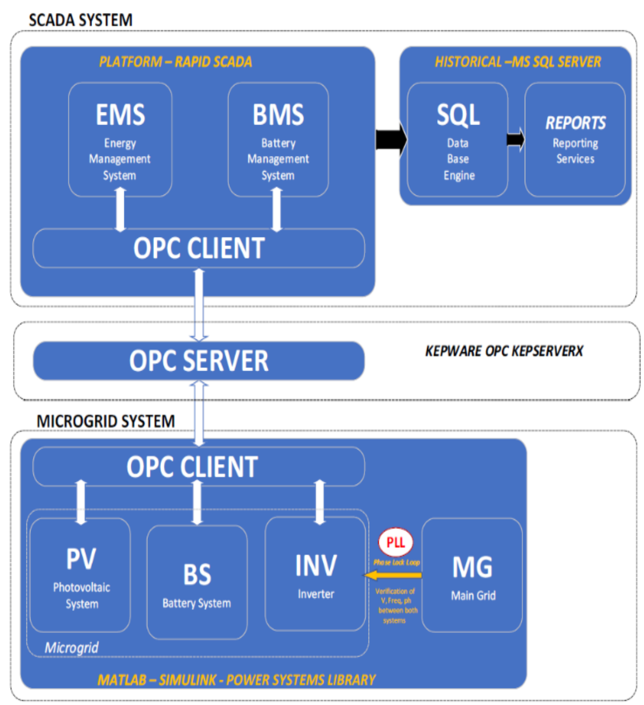

Fig. 1 Overview of the research proposal

A simulated environment, coupled with real-time communication capabilities, is critical for accurately modeling and testing the proposed Microgrid system. This ensures that the results generated are not only reliable but also transferable to real-world applications. As depicted in Figure 1, the development of the proposal is fundamentally based on the use of a simulated system within the Simulink platform, which acts as a representative microgrid model. In this configuration, an OPC server plays a crucial role as an intermediary, enabling seamless communication between the SCADA system and the simulated environment.

4.2. Microgrid System

- Solar panel system: This subsystem consists of an array of solar panels designed to generate up to 1000 Watts at peak performance;
- Battery System: The battery system includes a configuration of batteries with a total storage capacity of 50Ah, providing energy storage for the microgrid;
- Inverter: The inverter is responsible for converting the Direct Current (DC) generated by the solar panels and/or

the battery system into Alternating Current (AC), which is used to power standard electrical devices;

- External electrical network: This component represents the external electrical distribution system with which the microgrid may interface.

4.3. OPC Communication System

- OPC Server: Acts as the central hub for linking the data generated from the Microgrid simulation to other subsystems within the overall architecture;
- OPC Client - Simulink: This client communicates directly with the OPC server, transmitting the data generated from the Simulink-based simulation to the server;
- OPC Client -RapidSCADA: This client is responsible for receiving and processing the data transmitted to the OPC server by the Matlab OPC Client - Simulink (MATLAB OPC,2022).

4.4. Rapid SCADA System

The Rapid SCADA system is designed for data acquisition, visualization, and storage:

- Data acquisition: This component of the SCADA system captures and makes available the data collected from the OPC client (MATLAB OPC,2022);
- HMI: The HMI provides an intuitive and agile graphical interface that closely represents the real-world system, allowing for effective monitoring and control;
- History Subsystem: This subsystem is responsible for storing the data generated by the system and providing reporting services for analysis and record-keeping.

5. Microgrid System Implementation

5.1. Photovoltaic System or Solar Panel Arrangement

The photovoltaic system has been engineered to deliver a maximum power output of 1000 Watts under optimal conditions. As depicted in Figure 2, Simulink offers a specialized library that facilitates the accurate representation of this system.

This library allows straightforward configuration, enabling adjustments to achieve different voltage, current, and power outputs as required. The underlying assumption is that using such a configurable library not only simplifies the modeling process but also enhances the system's adaptability to various design specifications and simulation scenarios.

It is important to note that the simulation framework allows for the configuration of multiple solar panels connected in parallel or series. Additionally, key parameters such as open-circuit voltage and short-circuit current can be adjusted according to the specific characteristics of the panels being simulated. These capabilities ensure that the simulation accurately reflects the desired operational conditions of the photovoltaic system.

Moreover, the system provides a graphical representation of the solar panel array's current as a function of voltage, which can be easily generated using the Plot function. This feature is crucial for visualizing the performance characteristics of the simulated solar array.

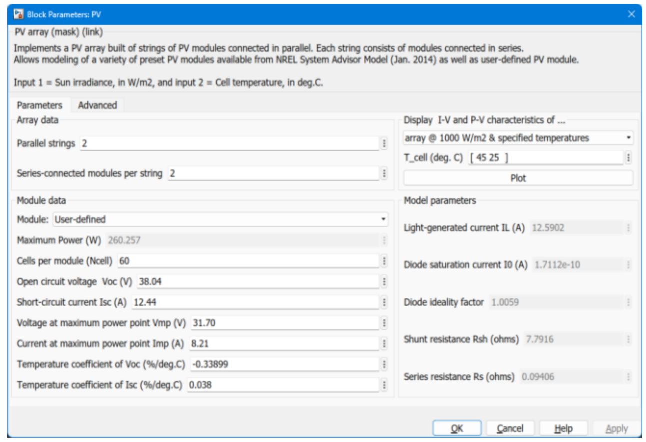

Fig. 2 Solar panel array configuration window

For this simulation, the HH180 solar panel's characteristics were employed as the basis for the model. It is crucial to emphasize that key input parameters solar irradiance W/m^2 and temperature ^oC play a significant role in determining the panel's power output. These parameters are critical as they directly influence the photovoltaic system's efficiency and overall performance. As illustrated in Figure 3, the simulation results provide a detailed visual representation of the power output under specified conditions of irradiance and temperature.

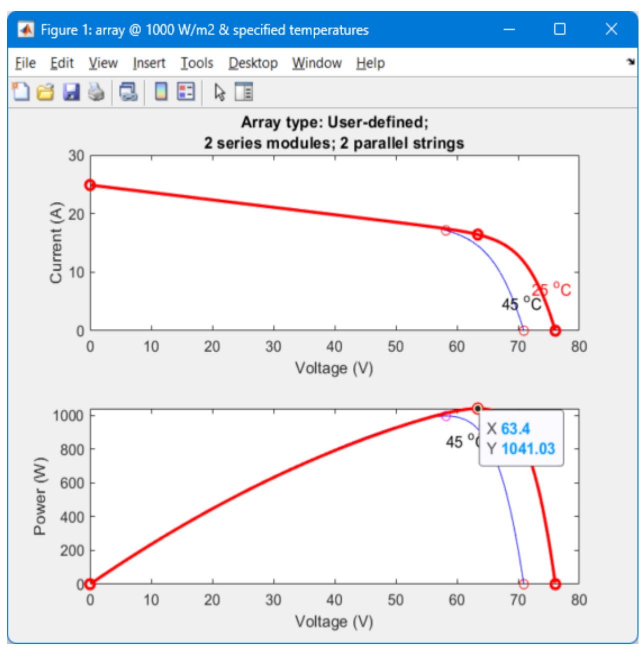

Fig. 3 Graphical representation of the solar panel array

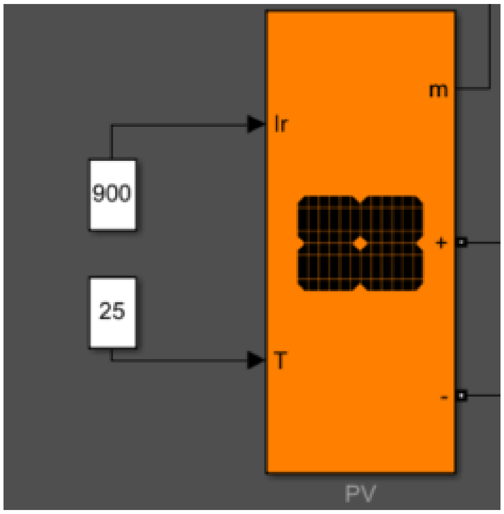

Fig. 4 Representation of the panel with its input parameters

In the context of Photovoltaic (PV) generation, the buck-boost converter plays a crucial role in managing the output voltage from the solar panel, adjusting it to meet the system's requirements. This converter can step up or down the output voltage relative to the input voltage, depending on the operating conditions.

This functionality is particularly important in PV systems, where the output voltage of the solar panel can vary significantly due to changes in solar irradiance and temperature. The buck-boost converter ensures that the system efficiently converts and utilizes the energy generated by the solar panels, regardless of environmental fluctuations.

The design process for such a converter was omitted here because it's irrelevant to the main goal of this study. The methodology for designing the solar panel system begins with calculating the standard and worst-case conditions for the solar panel arrangements, as detailed in Tables 3 and 4, which present the respective values found during this process.

Table 3. Standard conditions for the solar panel arrangement

Type	Description
Irradiation Standard	1000 W/m^2
Maximum Power	1000 W
Voltage at Maximum Power Point	63.4 V
Current at Maximum Power Point	16.42 A

Table 4. Worst-case conditions for the solar panel arrangement

Type	Description
Worst-Case Irradiation Condition	1000 W/m^2
Maximum Power	50 W
Voltage at Maximum Power Point	57.06 V
Current at Maximum Power Point	0.88 A

Following this, the switching frequency and voltage ripple are defined to ensure stable operation as f_s=25 KHz.

Next, the internal resistance of the solar panel array is determined at the maximum power point under both standard and worst-case scenarios.

$$\mathrm{R_{mps}} = \frac{\mathrm{V_{mps}}}{\mathrm{I_{mps}}} = \frac{63.4}{16.42} = 3.86\ \Omega \tag{1}$$

$$\mathrm{R_{mpw}} = \frac{\mathrm{V_{mpw}}}{\mathrm{I_{mpw}}} = \frac{57.06}{0.87} = 65.11\ \Omega \tag{2}$$

With these parameters in place, the output resistance is calculated using the following formula:

$$Ro = \left(0.2 \times R_{mps}\right) + \left(1.25 \times R_{mpw}\right) \tag{3}$$

$$Ro = (0.2 \times 3.86) + (1.25 \times 65.11) = 82.16\ \Omega$$

Subsequently, the duty cycle at the maximum power point is computed, followed by calculating the output voltage and current in both scenarios.

$$D_m = \frac{1}{1+\sqrt{\frac{R_{mp}}{R_o}}} \tag{4}$$

$$D_{mps} = \frac{1}{1+\sqrt{\frac{R_{mps}}{R_o}}} = \frac{1}{1+\sqrt{\frac{3.86}{82.16}}} = 0.82$$

$$D_{mpw} = \frac{1}{1+\sqrt{\frac{R_{mpw}}{R_o}}} = \frac{1}{1+\sqrt{\frac{65.11}{82.16}}} = 0.52$$

The process continues by calculating the output voltage and current in both scenarios:

$$\text{Output voltage: } V_o = \frac{-V_{mp}}{\frac{1}{D_{mp}}-1} \tag{5}$$

$$\text{Output current: } I_o = \frac{V_o}{R_o} \tag{6}$$

The inductor current, voltage ripple and current ripple are then calculated, which are essential for assessing the system's performance.

$$I_{LS} = \left|\frac{I_{os}}{1-D_{mps}}\right| = \left|\frac{-3.55}{1-0.82}\right| = 19.97\ A \tag{7}$$

$$\triangle V_{iw} = 0.02 \times V_{mpw} = 0.02 \times 57.06 = 0.114\ v \tag{8}$$

$$\triangle V_{ow} = 0.02 \times V_{ow} = 0.02 \times -64.06 = 0.128\ v \tag{9}$$

Finally, the values for C_i, L, and C_0 are obtained, completing the design process.

$$\boldsymbol{C_i = I_{LS} \times \frac{D_{mps}}{8 \times \triangle V_{iw} \times f_s} = 719.42\ uF} \tag{10}$$

$$\boldsymbol{C_i = I_{LS} \times \frac{D_{mps}}{8 \times \triangle V_{iw} \times f_s} = 719.42\ uF} \tag{11}$$

$$C_o = |I_{os}| \times \frac{D_{mps}}{8 \times \triangle V_{ow} \times f_s} = 15.72\ uF \tag{12}$$

With the circuit elements selected, they are integrated into the panel system previously generated solar:

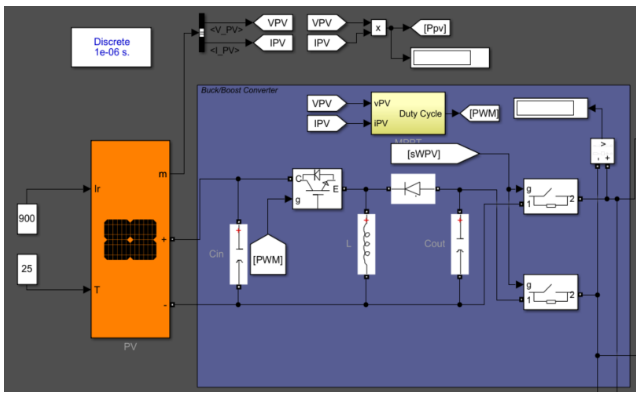

Fig. 5 Integrated Buck-Boost converter circuit

5.2. Maximum PowerPoint Tracking Algorithm Implementation

The Perturb and Observe (PO) algorithm was selected for its simplicity and ease of implementation, making it an efficient choice for Maximum Power Point Tracking (MPPT) in photovoltaic systems. The sequence of operations within the algorithm is depicted in the flowchart provided in Figure 6.

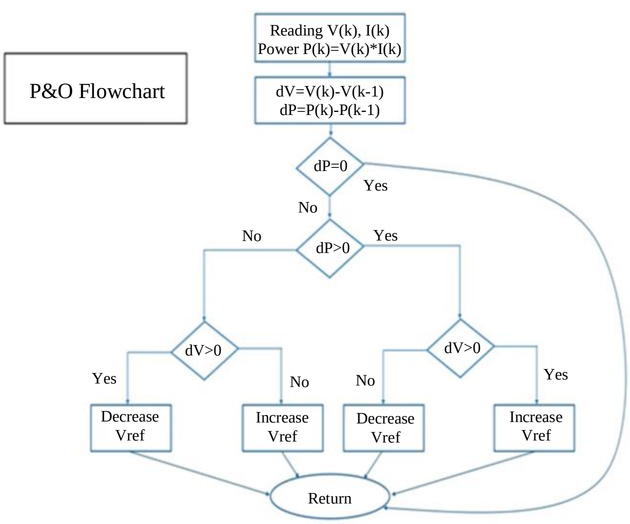

Fig. 6 Flowchart of the Perturb and Observe (PO) algorithm for Maximum Power Point Tracking

The algorithm uses three persistent variables: V_{old}, P_{old}, and $V_{ref(old)}$, which store the previous values of voltage, power, and reference voltage, respectively. These variables are essential for calculating the voltage (dV) and power (dP) variations between the current and previous iterations. If the algorithm is being executed for the first time, these variables are initialized with appropriate values (zero for V_{old} and P_{old}, and $V_{ref(init)}$ for $V_{ref(old)}$.

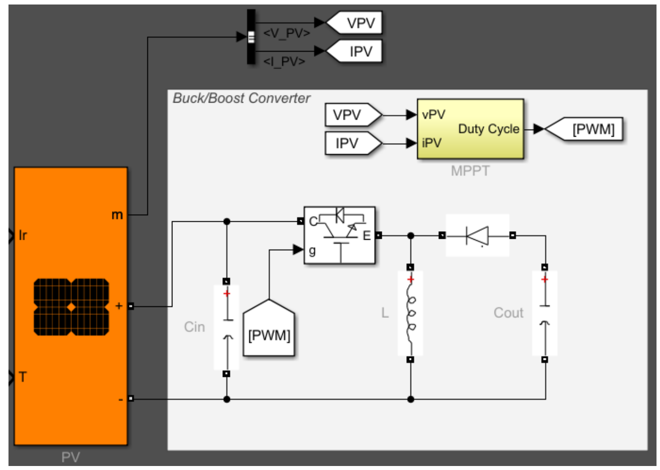

Fig. 7 MPPT controller in the Buck-Boost converter system

At each iteration, the algorithm calculates the instantaneous power generated by the solar panel using the product of the measured voltage (V) and the current (I) supplied by the panel: P = V. I. The variations in voltage ($dV = V - V_{old}$) and power ($dP = P - P_{old}$) compared to the previous iteration. These values are critical in determining how the algorithm should adjust the reference voltage to maximize power. As shown in Figure 7, which includes a representation of the solar panel, this mechanism is essential for maximizing energy generation efficiency and maintaining overall system stability. The core of the P&O algorithm is based on analyzing how the variations in power (dP) and voltage (dV) influence the adjustment of the reference voltage. The procedure follows conditional logic.

When power varies ($dP \neq 0$), if power decreases ($dP < 0$), and voltage has also decreased ($dV < 0$), the algorithm adjusts the reference voltage to a higher value, voltage ($V_{ref} = V_{ref(old)} - \Delta V_{ref}$) as this indicates that the MPP is at a higher voltage.

If the voltage has increased ($dV > 0$), the reference voltage is reduced voltage ($V_{ref} = V_{ref(old)} + \Delta V_{ref}$ to find the MPP at a lower voltage.

If power increases ($dP > 0$) and voltage decreases, the algorithm reduces the reference voltage ($V_{ref} = V_{ref(old)} - \Delta V_{ref}$), while if the voltage increases, it increases the reference voltage ($V_{ref} = V_{ref(old)} + \Delta V_{ref}$). The goal is to observe how power changes concerning voltage alterations.

If an increase in voltage results in an increase in power, the algorithm continues increasing the voltage until the MPPT is reached. Otherwise, it reverses the direction of the voltage adjustment. If the power does not vary (dP = 0), the algorithm maintains the previous reference voltage, assuming it is near the maximum power point.

After adjusting V_{ref}, the algorithm checks whether the adjusted value falls within the established limits ($V_{ref(max)}$ and $V_{ref(min)}$). If V_{ref} exceeds these limits, it is reset to the previous value ($V_{ref(old)}$), ensuring the system operates within a safe range. Finally, the algorithm updates the persistent variables V_{refold}, V_{old}, and P_{old} with the current values of V_{ref}, V, and P, respectively, ensuring that the next iteration has access to the necessary information for calculating voltage and power variations.

The control algorithm is integrated into a closed-loop system, which is realized through a MATLAB script. This system is designed to process two critical inputs: the current and voltage measurements from the solar panel array, and to generate a single output that regulates the system's operation. Specifically, the input signals, emphasising the voltage, are continuously monitored and compared with the output of the Perturb and Observe (P&O) algorithm. This comparison is essential for dynamically adjusting the operating point of the photovoltaic system, ensuring that it consistently tracks the maximum power point and optimizes energy harvesting efficiency. Integrating the P&O algorithm into this feedback mechanism is fundamental to achieving precise control over the system's performance.

Subsequently, the discrepancy between the measured input voltage and the output generated by the MPPT controller is processed by a Proportional-Integral (PI) controller. The PI controller is pivotal in minimizing this error by adjusting the system's response based on the present and accumulated errors over time. The PI controller's parameters were meticulously fine-tuned to achieve optimal system performance through a series of iterative tests and adjustments. This calibration process involved systematically refining the controller's gains to enhance stability, response time, and accuracy, as illustrated in Figure 8. The result is a robust control strategy that effectively maintains the photovoltaic system's operation at or near the maximum power point under varying conditions.

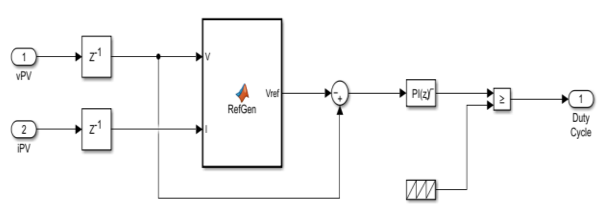

Fig. 8 Implementation of P& O algorithm

6. Single-Phase Inverter Design with PLL Anchoring to the External Grid

In the design of the inverter, a circuit comprising four MOSFET/IGBT transistors was employed to synthesize the AC signal, utilizing a Pulse-Width Modulation (PWM) control scheme. To suppress high-frequency noise generated by the rapid switching transients of the transistors, an LCL filter is implemented at the output stage, ensuring smoother signal quality and compliance with power quality standards.

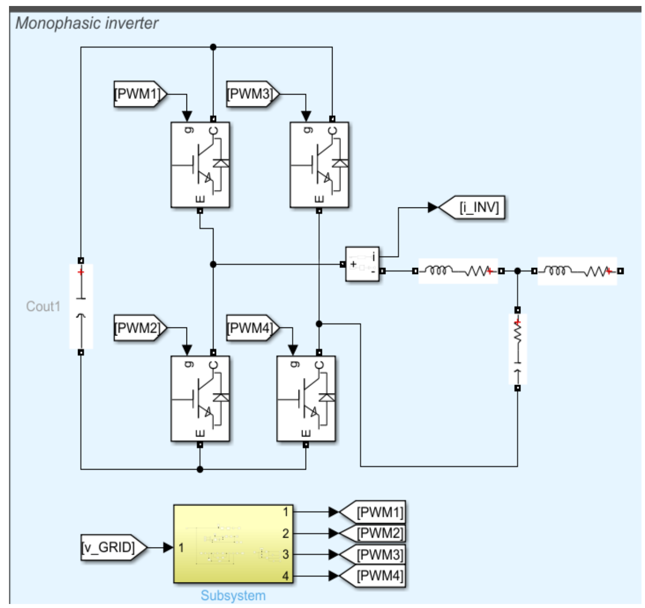

Fig. 9 DC/AC inverter circuit

6.1. LCL Filter Design

The first step involves calculating the capacitor value, which is determined by the amount of reactive power absorbed under nominal conditions.

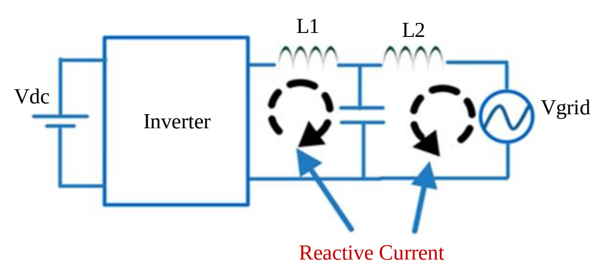

Fig. 10 LCL filter design

In this case, the reactive power (Q) is limited to 5% of the apparent power (S). The relationship is expressed by the equation:

$$Q = \frac{V^2}{0.5\times\pi\times f\times C} = 5\% \times S \tag{13}$$

$$C = \frac{0.05\times S}{V^2\times 2\times\pi\times f} = 5\% \times S \tag{14}$$

For our system, the values to be replaced would be:

$S = 500\, VA$

$V_{grid} = 70$

$f = 25KHz$

Therefore, the capacitor value would be C = 13.53 µF.

Next, the inductor value must be calculated. The inductor L_1 is selected based on the maximum permissible ripple in the current, which is limited to 20% of the nominal current.

$$L1 = \frac{V_{DC}}{4 \times F_{sw} \times I_{ppmax}} = 1.2\, mH \tag{15}$$

Additionally, the total inductance, represented as $L_1 + L_2$, is designed to ensure that the maximum voltage drop across the inductor does not exceed 10% of the nominal voltage.

$$L1 + L2 = 10\% \times \frac{V_{grid}}{\left(\left(\frac{S}{V_{grid}}\right) \times 2 \times \pi \times f\right)} = 2.6mH \tag{16}$$

Therefore, L2=1.4mH

Finally, a verification step is required for the calculated values. Using the reference frequency F_{res}, it is necessary to check if the following condition is met:

$$10 \cdot F_{grid} < F_{res} < 0.5 \cdot F_{sw} \tag{17}$$

The resonant frequency F_{res} is calculated,

$$F_{res} = \frac{1}{2\pi} \times \sqrt{\frac{(L1+L2)}{L1 \times L2}} = 1.7KHz \tag{18}$$

Comparing this with the given bounds:

600 < 1700 < 12500

It is confirmed that the condition holds true.

6.2. PLL System Design

A Phase-Locked Loop (PLL) system enables precise phase control of our system by synchronizing it with a reference signal. In our application, the microgrid system aims to remain in phase with the electrical grid, which serves as the reference.

The grid voltage is supplied as an input to the PLL system as part of the control strategy. The PLL then generates a reference current, which is compared with the inverter's output current to ensure phase alignment and proper synchronization with the grid. The operation of the PLL system is illustrated in Figure 11.

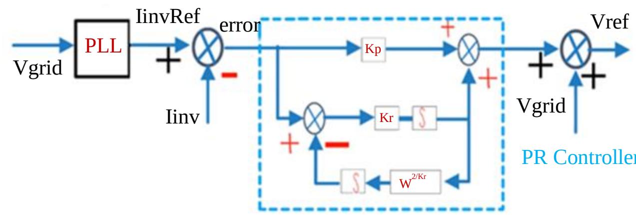

Fig. 11 Functional diagram of the grid-connected inverter

The PLL system begins by converting the voltage signal using the Alpha-Beta transformation. Once the Alpha-Beta signals are obtained, they transform into the dq reference frame, as illustrated in Figure 12.

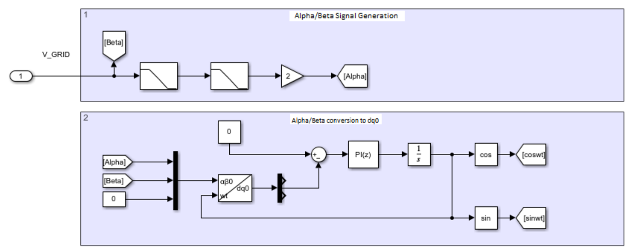

Fig. 12 Alpha-Beta to dq0 conversion

In the dq transformation block, only the q-component of the signal is used. When this signal is processed by a subsequently integrated PI controller, it provides the angle **Ω**t. By applying the cosine or sine functions to this angle, we obtain the following:

- cos(ωt): Active Current
- sin(ωt): Reactive current

Since our goal is to obtain the active current, we select (cos(ωt)) as the input signal for the PR controller. This signal is compared with the actual inverter current, and the resulting error is processed by the PR controller based on the selected gain values. To determine the controller constants, the values of the LCL filter must first be considered. The controller time constant is set at (T_s = 150 µ s). Using this value, we can calculate the proportional gain (K_P) as follows:

$$K_P = L_1/T_s = 7.9196 \tag{19}$$

Additionally, we choose a value of (k_r = 100).

Considering a frequency of 60 Hz, the gain can be calculated:

$$\frac{\omega_2}{k_r} = 1421.2 \tag{20}$$

These values will be input into our PR controller. Consequently, we obtain the reference voltage V_{ref}, which will be used as the input for the PWM generation block, as illustrated in Figures 13 and 14.

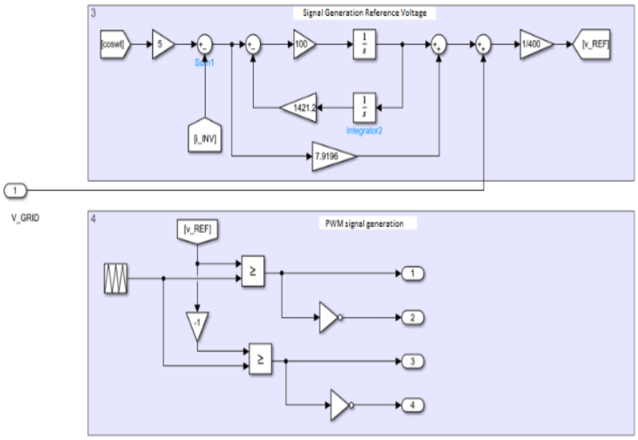

Fig. 13 PWM signal generation for IGBT gates

The reference voltage will be used to generate 4 PWM signals that feed the 4 IGBT gates that are part of the inverter, as illustrated in Figures 13 and 14.

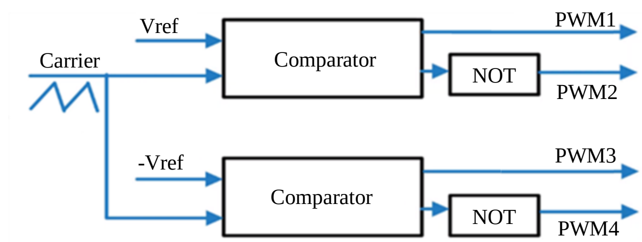

Fig. 14 PWM signal generation scheme

7. Electrical Network

The electrical network was simulated using a 220 V generator operating at 60 Hz with an 80 Ω load. For the purposes of the simulation, a purely active load was assumed, resulting in a power factor of 1, as illustrated in Figure 15.

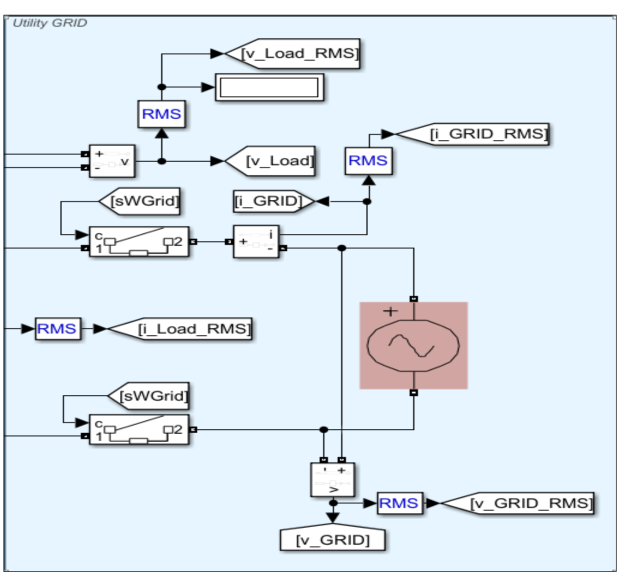

Fig. 15 Simulation of the load and the electrical network

8. OPC Communication

Matlab has an OPC client, which allows communication with an OPC server, as shown in Figure 16. This client will be in charge of transmitting the information to our SCADA server.

The OPC server used is the Kepware KepServerEx *v*6.14, which, in its freeware version, is fully functional. Its limitation in the freeware version is that after 1 hour of use, it must be restarted (KEPServerEX - KEPinfilink, n. d.). The OPC communication maintains the following communication architecture:

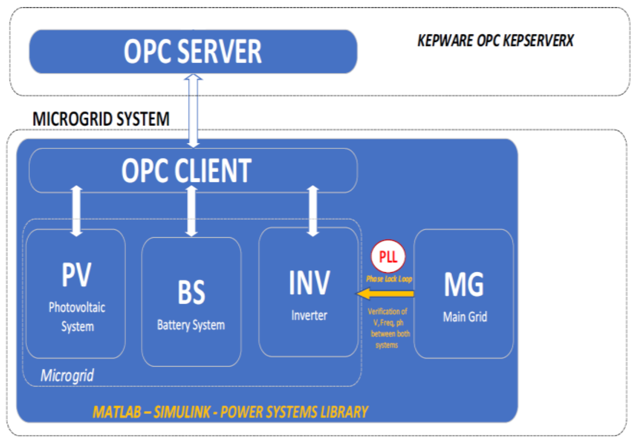

Fig. 16 OPC Server and Matlab communication architecture (Own elaboration)

In Matlab, the configuration is simple, and it is only necessary to enter the OPC server's connection text Figure 17.

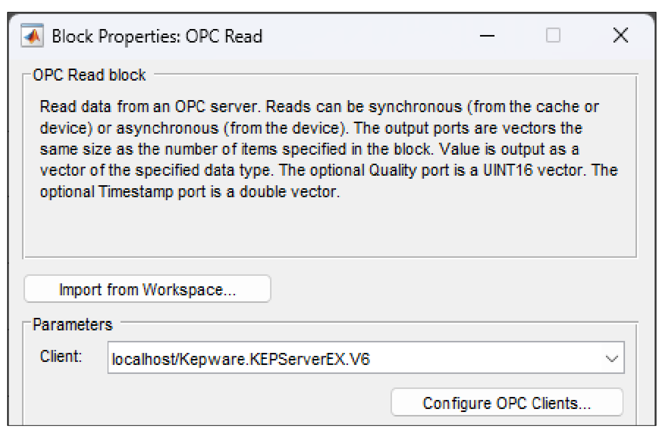

Fig. 17 Matlab OPC client configuration

Once the connection text has been set, it is possible to map the tags available on the OPC server (previously created). Tags can be created from the Kepware server configuration Windows in Figure 18. Each tag corresponds to the following Tables 5 and 6. Figure 19 shows the captured values and the "Good" status as a quality flag, which confirms that the information received is correct.

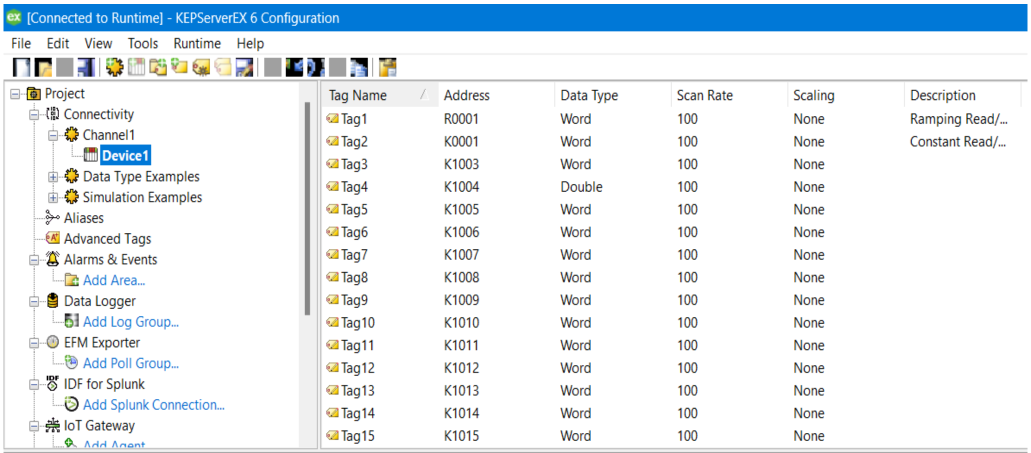

Fig. 18 Tag creation and configuration window

Table 5 .Analog signals (Own elaboration)

Analog Signals				
TAG	**Sign**	**Unit**	**Type**	**Commentary**
1	SOC (State of Charge) - Battery	%	Read	Battery charge status
2	Voltage - Battery	V	Read	Voltage (at the battery)
3	Current - Battery	A	Read	Current (in battery)
4	Solar Radiation	W/m2	Read	Solar radiation
5	Temperature	°C	Read	Temperate
6	Power - Solar Panel	W	Read	Power (at panel output)
7	Voltage - Solar Panel	V	Read	Voltage (at panel output)
8	Corriente - Solar Panel	A	Read	Current (At panel output)
9	Voltage - Utility	V	Read	Voltage (At the power grid output)
10	Current - Utility	A	Read	Current (At the power grid output)
11	Voltage - House	V	Read	Voltage (At the entrance of the home/residence)
12	Current - House	A	Read	Current (At the entrance of the home/residence)
13	Voltage - Inverter	V	Read	Voltage(At inverter output)
14	Current - Inverter	A	Read	Current (At inverter output)
15	Energy consumed	KwH	Read	KiloWatt-Hour (At the entrance of the home/residence) **Calculated from the power and the elapsed time
16	Injected energy	KwH	Read	KiloWatt-Hour (At the entrance of the home/residence) ** Calculated from the power and the elapsed time

Table 6 .Digital signals (own elaboration)

Digital Signs				
TAG	**Sign**	**Unit**	**Type**	**Commentary**
17	MCB Position- Panel	ON/OFF	Read/Write	MCB Mini Circuit Breaker
18	MCB Position- Battery Input	ON/OFF	Read/Write	MCB Position - Battery Input
19	MCB Position- Battery Output	ON/OFF	Read/Write	MCB Position - Battery Output
20	MCB Position- Inverter Input - Battery	ON/OFF	Read/Write	MCB Position - Inverter Input - Battery
21	MCB Position- Inverter Input - Solar Panel	ON/OFF	Read/Write	MCB Position - Inverter Input - Solar Panel
22	MCB Position- Inverter Output	ON/OFF	Read/Write	MCB Position - Inverter Output
23	MCB Position- Power Grid	ON/OFF	Read/Write	MCB Position - Power Grid

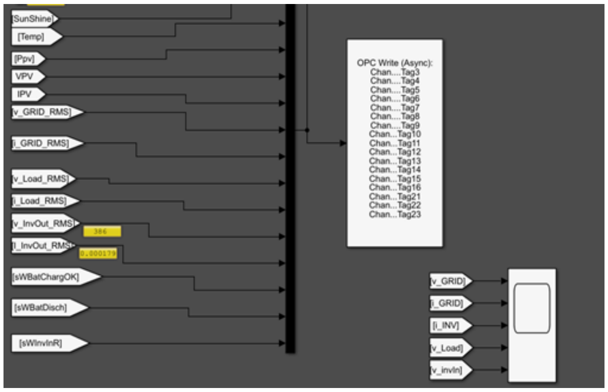

Fig. 19 OPC communication block

9. RapidSCADA Server

RapidSCADA is an open-source platform for industrial automation. It contains several modules and tools that allow the rapid creation of control and monitoring systems.This platform is installed on Windows and Linux operating systems. The minimum requirement is for Microsoft Windows 7 SP1 or Microsoft Windows Server R2 with Internet Information Services (IIS) enabled, in addition to the platform .NET 4.7.2. Once the platform is installed, proceed to make the configurations for communication. The main ones are the following:

- Creation of communication line: The type of communication is defined, either serial or IP, as well as the communication driver.
- Device creation: The communication parameters are defined according to the established protocol.
- Tag creation: The signals to be communicated are defined as either input (read) or output (write).

Figure 20 shows the OPC - RapidSCADA client configuration window.

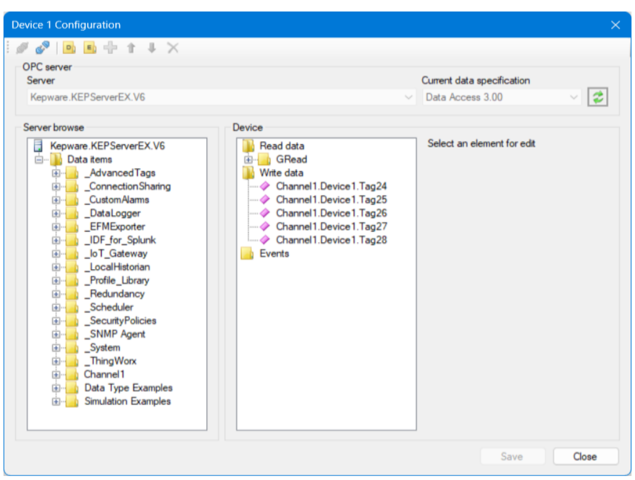

Fig. 20 OPC - RapidSCADA client configuration window

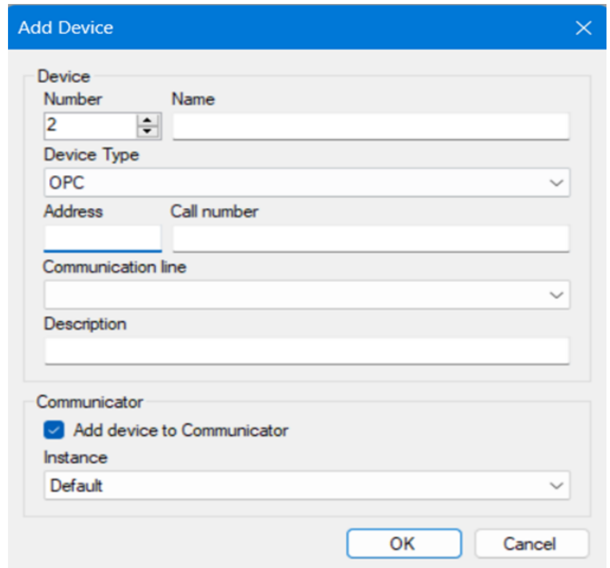

Fig. 21 Device creation window

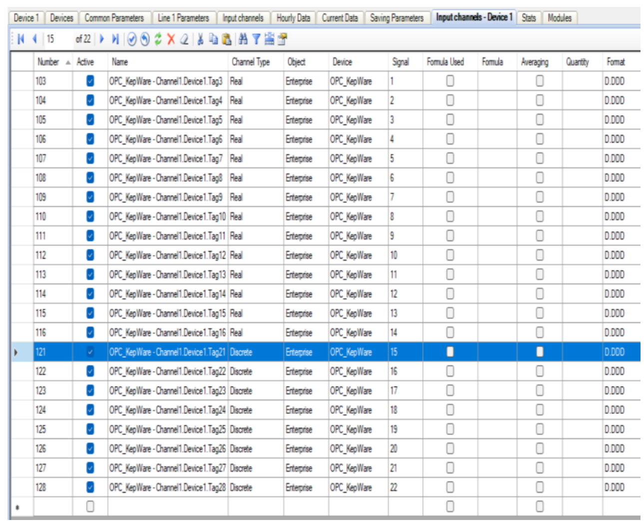
Fig. 22 Tags or signals configuration window (Own elaboration)

Figure 21 shows the device creation window. Figure 22 shows the tags or signals configuration window. Once the signals have been configured, we proceed to the configuration of the graphical part of the SCADA. Two types of displays will be used: tables and diagrams. The tables, as their name indicates, correspond to the presentation of the information in rows and columns according to the variable and the value. Diagrams present the information using a graphical representation of the system to be monitored.

The diagrams are created with the Rapid SCADA editing tool supported by a web browser, from where you can easily observe how the display will look. Figure 23 shows the data table, Rapid SCADA deployment. Figure 24 shows the Rapid Scada, showing the values in real time.

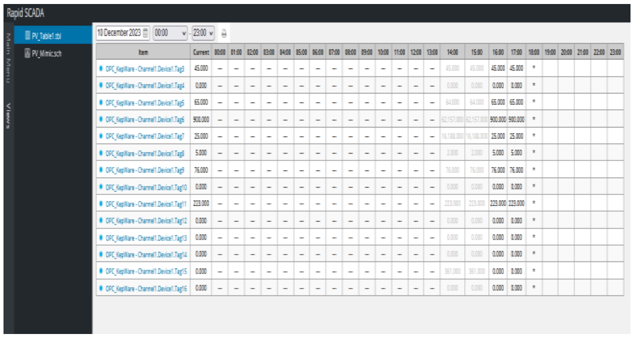

Fig. 23 Data table, Rapid SCADA deployment

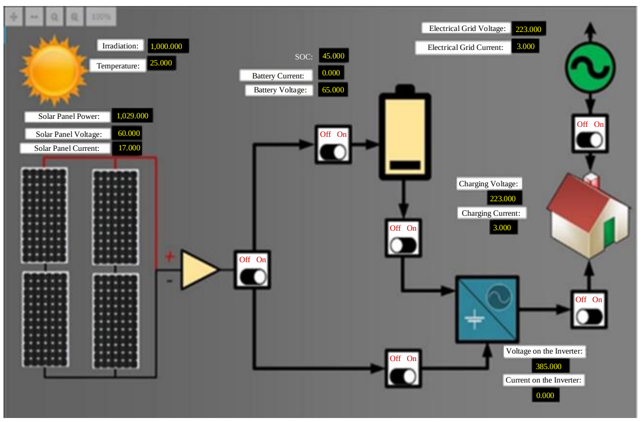

Fig. 24 Rapid Scada Server (Own elaboration)

10. SQL Server and Reporting Services

An important part of the SCADA system is the ability to access previous records in order to review past information that, in a given situation, could be useful to us. For this, we used an external database, the express version of MS SQL, which is free and has the necessary functionality to meet the objectives of our system.

MS SQL Express is available on Microsoft's official website, the installation is simple and is done in a few steps. What is important is to define the name, or instance of the database, i.e. how the database will recognize a request made from an external client to it. In our case, we modified the MS SQL instance so that it can be recognized only with the IP address of the host computer.

Figure 25 shows the alias configuration for MSSQL Instance. Once the instance is initialized and the SQL service works correctly, a structure that will house our data must be created. A flat table was used in this case, considering the time stamp as the main column. Figure 26 shows the MS SQL history table. With our structure created, we must activate the Rapid SCADA database module. Here, we place the main communication parameters and then the sentence that will insert the data into the table previously created. Figure 27 shows the Rapid SCADA writing module configuration in the Database.

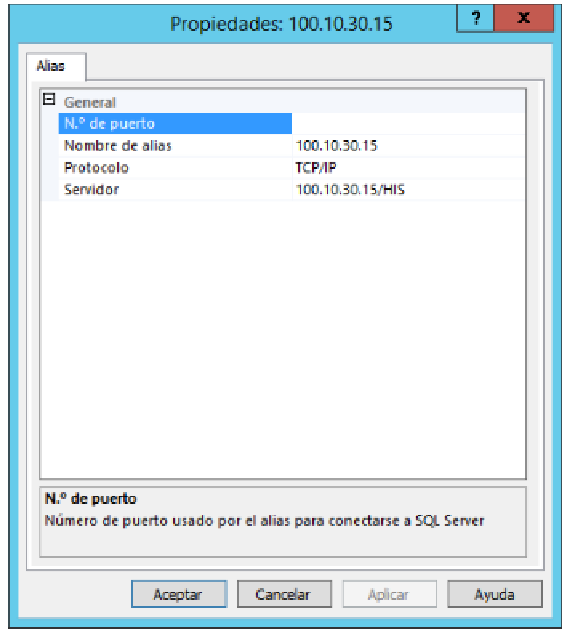

Fig. 25 Alias Configuration for MSSQL instance

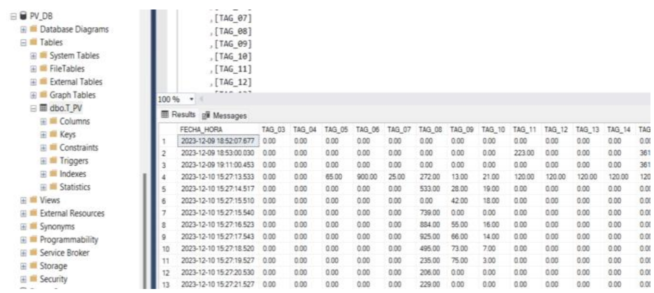

Fig. 26 MS SQL history table

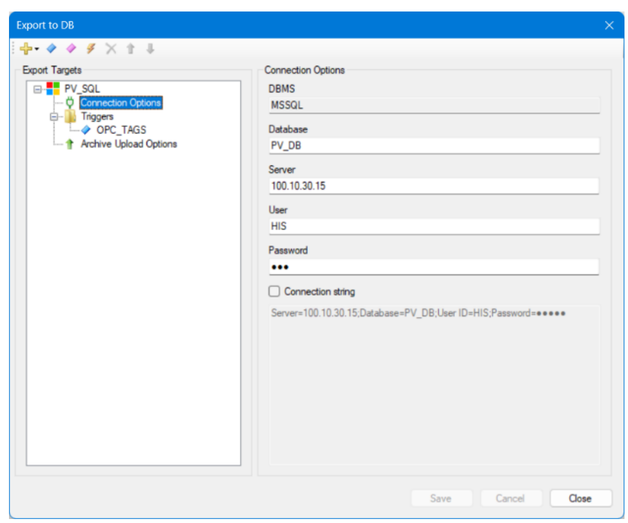

Fig. 27 RapidSCADA writing module configuration in database

Figure 28 shows the data insertion screen in the SQL instance. The whole statement was created using SQL language. As seen in the Figure 29 it inserts the instantaneous values at a certain time in the previously created table.

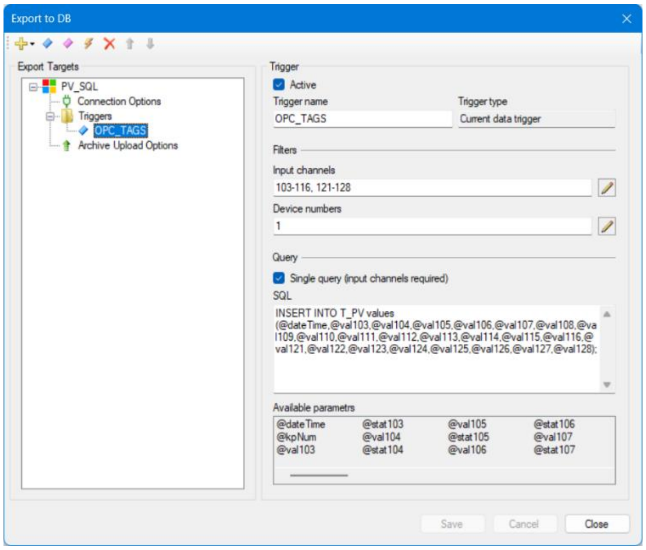

Fig. 28 Data insertion screen in SQL instance

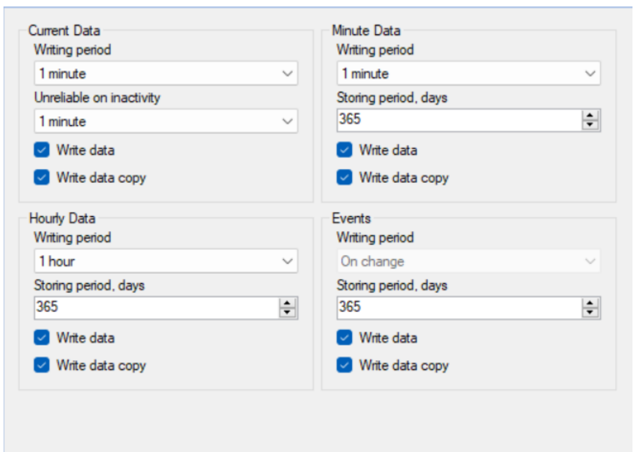

Fig. 29 Data writing configuration in RapidSCADA

Having made our data storage structure, we will now proceed to configure the reports. A report is a customized representation of the stored data. Using Microsoft's Reporting Services, which is also free of charge, we can access the data stored in the database from a web server.

Reporting Services also uses its own database for its configuration, which should not be confused with the previously created database. A SQL instance and an operating system with IIS are prerequisites. With the reporting service installed, it is also necessary to have the Report Builder tool, distributed free of charge on the Microsoft website.

Figure 30 shows the reporting services configuration window. Since the reporting system is a client of SQL Server, a connection text similar to the one created in Rapid SCADA is required. Figure 31 shows the reporting services configuration window for access to the SQL server.

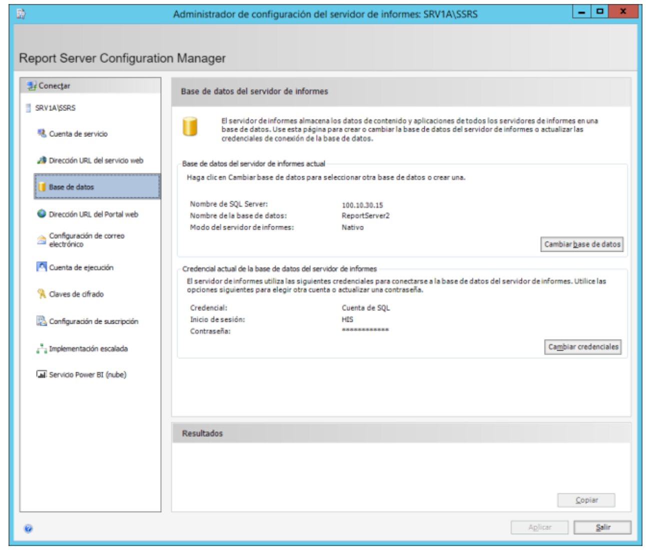

Fig. 30 Reporting services configuration window

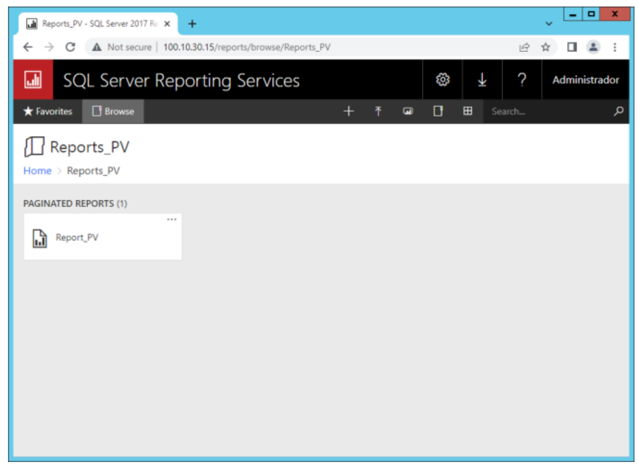

Fig. 31 Reporting services welcome screen

Since the reporting system is a client of SQL Server, a connection text similar to the one created in Rapid SCADA is required. Figure 32 shows the reporting services configuration window for access to the SQL server.

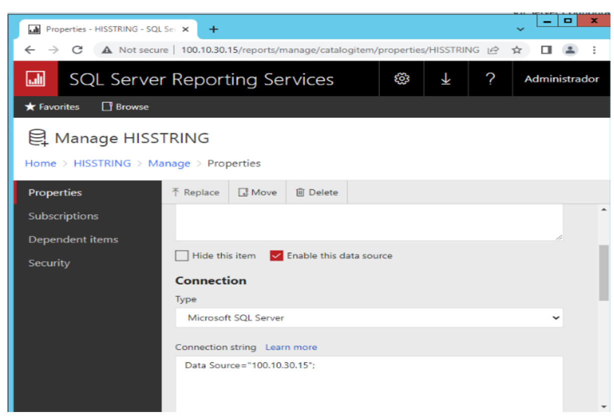

Fig. 32 Reporting services configuration window for access to the SQL server

This way, we will have access to the data stored in the table we previously created. Once this step is done, it is possible to create the report as such. To do this we use the same web interface, which will automatically take us to the Report Builder to construct the report. Figure 33 shows the Report Builder configuration window.

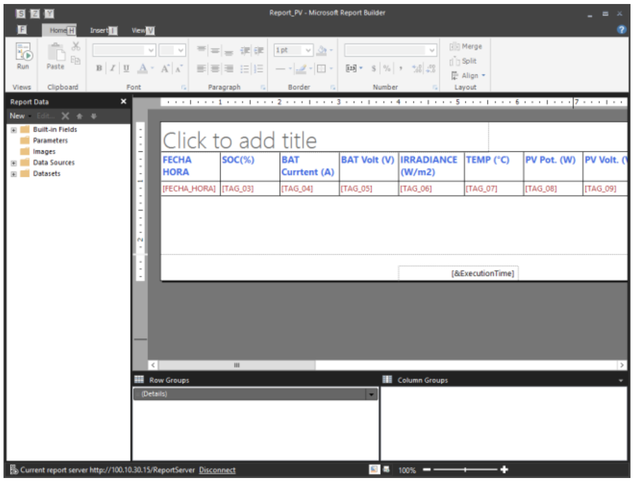

Fig. 33 Report builder configuration window

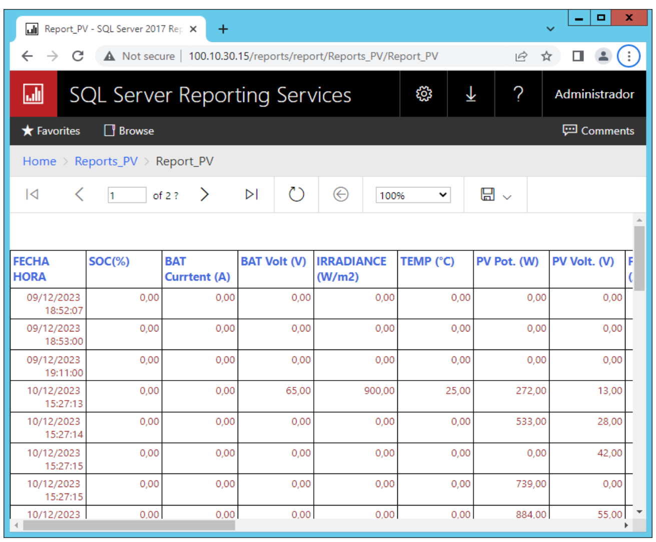

FECHA HORA	SOC(%)	BAT Currtent (A)	BAT Volt (V)	IRRADIANCE (W/m2)	TEMP (°C)	PV Pot. (W)	PV Volt. (V)
09/12/2023 18:52:07	0,00	0,00	0,00	0,00	0,00	0,00	0,00
09/12/2023 18:53:00	0,00	0,00	0,00	0,00	0,00	0,00	0,00
09/12/2023 19:11:00	0,00	0,00	0,00	0,00	0,00	0,00	0,00
10/12/2023 15:27:13	0,00	0,00	65,00	900,00	25,00	272,00	13,00
10/12/2023 15:27:14	0,00	0,00	0,00	0,00	0,00	533,00	28,00
10/12/2023 15:27:15	0,00	0,00	0,00	0,00	0,00	0,00	42,00
10/12/2023 15:27:15	0,00	0,00	0,00	0,00	0,00	739,00	0,00
10/12/2023	0,00	0,00	0,00	0,00	0,00	884,00	55,00

Fig. 34 Data report via web

With the Report Builder, we will give shape to the collected data; since it is a simple data structure, we will choose a table as a representation. With the report built, it is accessed through the web interface, and we can see the stored data. Figure 34 shows the data report via the web. Thus, we completed the process of data submission and monitoring of our SCADA system.

11. Results and Discussion

11.1. Performance Evaluation

The SCADA system's performance was evaluated through simulations. Results indicate efficient energy management, with error margins below 5% under varying conditions. Comparative analyses show that our system reduces implementation costs by up to 40% compared to proprietary solutions.

11.2. User Feedback

Survey results from potential users highlight the system's intuitive interface and adaptability. Stakeholders emphasized its potential to address energy challenges in rural areas.

11.3. Limitations

While the system demonstrates robust functionality, scalability to larger microgrids requires further investigation. Future work will focus on addressing these limitations.

12. Conclusion

This study presents a cost-effective, open-source SCADA system for microgrid management, addressing critical barriers to renewable energy adoption in developing regions. Its modular design and adaptability offer significant advantages over existing solutions, fostering sustainable energy independence. Future research will explore scalability and educational initiatives to enhance technology adoption. This article successfully simulated a microgrid using the environment Matlab Simulink, considering the data capture subsystems' energy, storage, and connection to the electrical grid.

The SCADA system was developed in an open-source environment, without resulting in cost, which encourages using these solutions for applications where the economic factor is determining to carry out the cape. The systems licensed in their express version were sufficient to complete the application; since the microgrid information does not require more robust solutions, they are presented as reliable alternatives and viable for real applications. The auxiliary history and reporting systems were configured correctly, managing to store the information generated by the microgrid for later reference. It was possible to correctly integrate the various systems that make up the final application, demonstrating that it is possible to use SCADA applications to monitor and control microgrids without incurring additional costs and stimulating its use and massification. The home consumption was characterized, and it was shown that the investment in solar energy can be recovered between 1 and 2 years, depending on the power acquired. The RapidSCADA solution complements these systems by providing a fast and effective monitoring method without representing an additional cost.

Acknowledgements

The authors express their sincere gratitude to the Universidad Nacional de San Agustín de Arequipa for their invaluable support and collaboration throughout the research process.

References

[1] Rafael Espinoza et al., Barriers to Overcome in the Attempt of a Massive Intervention of Grid-Connected PV Systems in Peru," *Tecnia*, vol. 27, no. 1, pp. 7-13, 2017. [CrossRef] [Google Scholar] [Publisher Link]

[2] Carlos Vargas-Salgado et al., "Low-Cost Web-Based Supervisory Control and Data Acquisition System for a Microgrid Testbed: A Case Study in Design and Implementation for Academic and Research Applications," *Heliyon*, **vol.** 5, no. 9, 2019. [CrossRef] [Google Scholar] [Publisher Link]

[3] Ertuğrul Adigüzel, Koray Gürkan, and Aysel Ersoy, "Design and Development of Data Acquisition System (DAS) for Panel Characterization in PV Energy Systems," *Measurement*, vol. 221, 2023. [CrossRef] [Google Scholar] [Publisher Link]

[4] Aslan Gholami et al., "Electrical, Thermal and Optical Modeling of Photovoltaic Systems: Step-by-Step Guide and Comparative Review Study," *Sustainable Energy Technologies and Assessments*, vol. 49, 2022. [CrossRef] [Google Scholar] [Publisher Link]

[5] Shuangshuang Li et al., "Research and Application of a SCADA System for a Microgrid," *Technologies*, vol. 5, no. 2, 2017. [CrossRef] [Google Scholar] [Publisher Link]

[6] Peter Loshin, Tech Target, SCADA (Supervisory Control and Data Acquisition), 2021. [Online]. Available: https://www.techtarget.com/whatis/definition/SCADA-supervisory-control-and-data-acquisition

[7] Matlab, Simulink for Model-Based Design, Mathworks, 2022. [Online]. Available: https://la.mathworks.com/products/simulink.html

[8] Ministry of Energy and Mines, Guidance on Efficient Use of Energy and Energy Diagnosis in Sectors. [Online]. Available: https://www.gob.pe/institucion/minem/colecciones/25400-guias-de-orientacion-del-uso-eficiente-de-la-energia

[9] Matlab, OPC Standards Communication, MATLAB and Simulink - MathWorks, 2022. https://la.mathworks.com/help/icomm/opc.html.

[10] G.O. Young, *Synthetic Structure of Industrial Plastics*, 2nd Ed, McGraw-Hill, New York, pp. 15-64, 1964. [Google Scholar]

[11] W.K. Chen, *Linear Networks and Systems*, Belmont. Wadsworth, Boston, pp. 123-135, 1993.

[12] J.U. Duncombe, "Infrared Navigation-Part I: An Assessment of Feasibility," *IEEE Transactions on Electron Devices*, vol. 11, no. 1, pp. 34-39, 1959. [Google Scholar]

[13] E.P. Wigner, "Theory of Traveling-Wave Optical Laser," *IEEE Transactions on Antennas and Propagation*, vol. 134, pp. A635-A646, 1965. [Google Scholar]

[14] H. Kurss, and W. Kahn, "A Note on Reflector Arrays," *IEEE Transactions on Antennas and Propagation*, vol. 15, no. 5, pp. 692-693, 1967. [CrossRef] [Google Scholar] [Publisher Link]

[15] Earl E. Reber, Richard L. Michell, and Clarence J. Carter, "*Oxygen Absorption in the Earth's Atmosphere*," Technical Report, Aerospace Corp El Segundo Calif Lab Operations, Los Angeles, CA, USA, 1988. [Google Scholar] [Publisher Link]

[16] J.H. Davis, and J.R. Cogdell, "*Calibration Program for the 16-Foot Antenna*," Electrical Engineering Research Lab, Texas University, Austin, 1987. [Google Scholar]

[17] Members of the Technical Staff Bell Telephone Laboratories, *Transmission Systems for Communications*, 3rd ed., Western Electric Company, Inc., Winston-Salem, NC, USA, 1985.

[18] W.P. Risk, G.S. Kino, and H.J. Shaw, "Fiber-Optic Frequency Shifter Using a Surface Acoustic Wave Incident at an Oblique Angle," *Optics Letters*, vol. 11, no. 2, pp. 115-117, 1986. [CrossRef] [Google Scholar] [Publisher Link]